

## CHEMODYNAMICAL SIMULATIONS OF ELLIPTICAL GALAXIES

Brad K. Gibson<sup>1</sup>, Patricia Sánchez-Blázquez<sup>1</sup>, Stéphanie Courty<sup>1</sup> and  
Daisuke Kawata<sup>2</sup>

**Abstract.** We review recent developments in the field of chemodynamical simulations of elliptical galaxies, highlighting (in an admittedly biased fashion) the work conducted with our cosmological N-body/SPH code `GCD+`. We have demonstrated previously the recovery of several primary *integrated* early-type system scaling relations (e.g. colour-magnitude relation,  $L_X$ - $T_X$ - $[\text{Fe}/\text{H}]_X$ ) when employing a phenomenological AGN heating scheme in conjunction with a self-consistent treatment of star formation, supernovae feedback, radiative cooling, chemical enrichment, and stellar/X-ray population synthesis. Here we emphasise characteristics derived from the full *spatial* information contained within the simulated dataset, including stellar and coronal morphologies, metallicity distribution functions, and abundance gradients.

### 1 Introduction

Our understanding of the formation and evolution of elliptical galaxies is undergoing something of a renaissance. The comfortable classical hierarchical merging scenario in which massive ellipticals form later than their less massive counterparts, faces challenges when confronted with empirical evidence for the existence of old, metal-rich, proto-ellipticals at redshifts  $z \approx 2 \rightarrow 3$ . The concepts of 'downsizing' (in which stars in more massive galaxies form earlier and on a shorter timescale than in less massive systems) and 'dry mergers' (dissipationless merging of stellar systems, without associated star formation) have proven to be popular enhancements to the conventional picture, although both face challenges in the face of the constraints imposed by known correlations in optical (e.g. colour-magnitude, luminosity-metallicity, Fundamental Plane) and X-ray (e.g. luminosity-temperature-metallicity) properties.

---

<sup>1</sup> University of Central Lancashire, Centre for Astrophysics, Preston, PR1 2HE, United Kingdom; e-mail: [bkgibson@uclan.ac.uk](mailto:bkgibson@uclan.ac.uk) & [psanchez-blazquez@uclan.ac.uk](mailto:psanchez-blazquez@uclan.ac.uk) & [scourty@uclan.ac.uk](mailto:scourty@uclan.ac.uk)

<sup>2</sup> Carnegie Observatories, Pasadena, USA; e-mail: [dkawata@ociw.edu](mailto:dkawata@ociw.edu)

While the semi-analytical methodology remains powerful when exploring both monolithic (e.g. Gibson 1997) and merger-driven (e.g. Pipino *et al.* 2006) frameworks for galaxy formation, the computational approach has progressed to the stage where fully coupled multi-wavelength spectro-chemical + dynamical simulations of ellipticals are now feasible. For example, the origin of optical scaling relations and abundance gradients has been explored recently by Kobayashi (2004), within the idealised context of semi-cosmological initial conditions, while the power of fully cosmological hydrodynamic simulations, which neglect both supernovae and AGN feedback, has been demonstrated by Domínguez-Tenreiro *et al.* (2006) and Naab *et al.* (2006). Recent cosmological simulations which include treatments of feedback include those of Meza *et al.* (2003),<sup>1</sup> Sommer-Larsen *et al.* (2003),<sup>2</sup> and Kawata & Gibson (2005, and references therein).

Kawata & Gibson (2005) studied the effect of AGN heating on the chemodynamical evolution of ellipticals, including the impact on both the integrated optical (e.g. colour-magnitude relation) and X-ray (e.g. luminosity-temperature-metallicity relations) properties. Driven by central convergent gas flows, the self-regulating nature of AGN heating within the Kawata & Gibson simulation leads to a stable hot corona and the suppression of late-time star formation. The cosmological elliptical simulated was shown to be consistent with these observed integrated properties.

## 2 New Results

Instead of repeating the discussion of Kawata & Gibson (2005), in what follows we report on our recent work in assessing the success (and failure) of our current suite of simulations in recovering various spatially-resolved optical and X-ray observables. This report is very much a work-in-progress, but should provide the reader with an overview of the direction in which we are heading.

### 2.1 Morphology

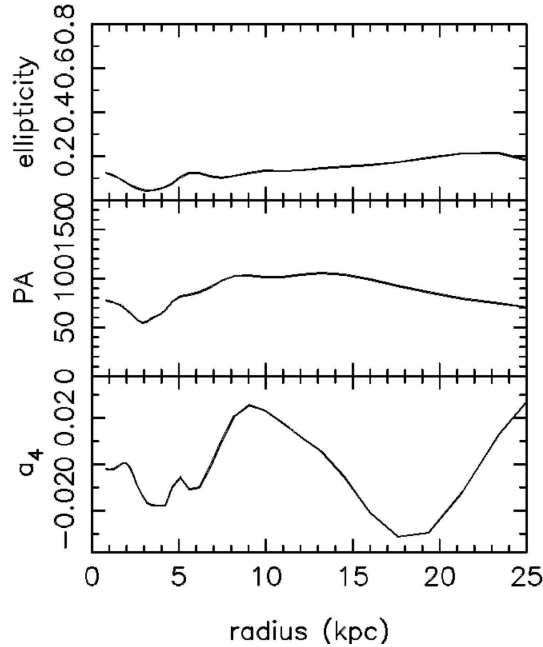
Our reference simulation here corresponds to Model 2 of Kawata & Gibson (2005), a mildly triaxial, slow oblate rotator, whose central line-of-sight velocity dispersion  $\sigma$  and rotation velocity  $V_{\text{rot}}$  match those of, for example, NGC 3379 ( $\sim 50$  km/s and  $\sim 250$  km/s, respectively).<sup>3</sup> Making use of its simulated optical isophotes, we measured the  $m=4$  deviations from perfect ellipses (the so-called  $a_4$  parameter). Viewed at high-inclination the galaxy can be characterised as possessing disk ( $a_4 > 0$ ) isophotes over the range  $0.5 \lesssim R/R_{\text{eff}} \lesssim 1.5$ , and boxy ( $a_4 < 0$ ) isophotes beyond  $R/R_{\text{eff}} \approx 2$  (see Fig 1), consistent with that found by Meza *et al.* (2003;

---

<sup>1</sup>Neglecting AGN feedback.

<sup>2</sup>Neglecting AGN feedback, Type Ia supernovae, and metallic line cooling.

<sup>3</sup>Admittedly though, the simulated galaxy's effective radius is  $\sim 11$  kpc, while that of NGC 3379 is  $\sim 2$  kpc.



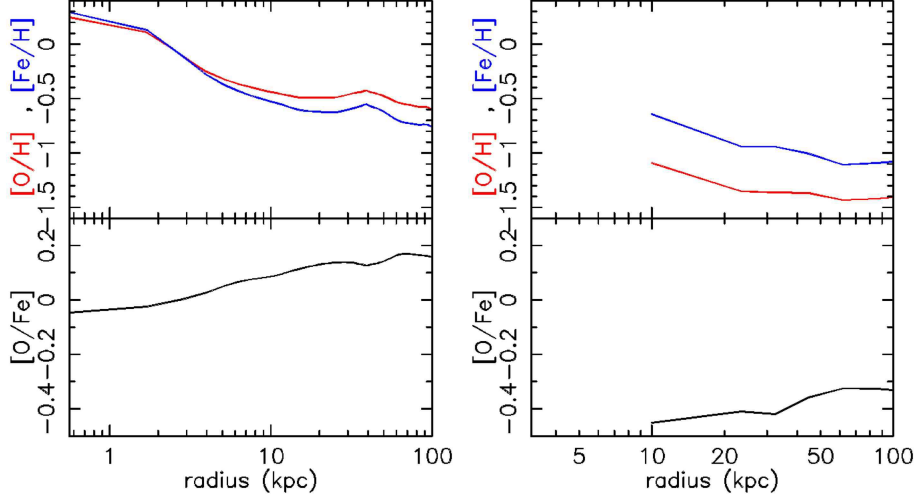
**Fig. 1.** Ellipticity, position angle, and  $m=4$  deviations from perfect ellipses (top to bottom panels, respectively) for Model 2 of Kawata & Gibson (2005), as viewed in projection at high-inclination.

Fig 11;  $50^\circ \lesssim \theta \lesssim 70^\circ$ ) for their cosmological elliptical galaxy simulation, and the disk isophotes observed within the effective radius of NGC 3379.

Diehl & Statler (2006) have recently suggested that the hot coronal gas within  $R/R_{eff} < 2$  and the underlying stellar components of ellipticals appear to have broadly aligned position angles, but the ellipticities are not well-correlated, as might be expected in hydrostatic equilibrium. We attempted to confront our simulations with this Chandra-inspired empirical evidence by fitting ellipses to the X-ray contour maps of our reference simulation; unfortunately, insufficient resolution compromised our ability to do so. It is clear though that the next-generation of simulations will be ideally suited for this problem (Gottlöber *et al.* 2006).

## 2.2 Gradients

In the upper (left) panel of Fig 2, we show the light-weighted iron (blue) and oxygen (red) abundance gradients for the stellar component of Kawata & Gibson's (2005) Model 2; the bottom (left) panel shows the corresponding abundance ratio ([O/Fe]) gradient. Near the effective radius, the gradients in [Fe/H] and [O/Fe]



**Fig. 2.** *Left:* Stellar abundance (upper) and abundance ratio (lower) gradients for Model 2 of Kawata & Gibson (2005). *Right:* X-ray coronal abundances (upper) and abundance ratio (lower) gradients for the same simulation.

are  $d\langle[Fe/H]\rangle/d(\log r)\approx-0.3$  and  $d\langle[O/Fe]\rangle/d(\log r)\approx+0.1$ , respectively. The agreement with the gradients derived by Sánchez-Blázquez et al. (2006)<sup>4</sup> for NGC 3379 ( $d\langle[Fe/H]\rangle/d(\log r)\approx-0.30$  and  $d\langle[O/Fe]\rangle/d(\log r)\approx+0.04$ , respectively) is re-assuring (and admittedly, perhaps a coincidence) and consistent with the similarity found between the morphology of NGC 3379 and our reference model (§ 2.1). Our simulated elliptical is consistent with the predictions of "outside-in" scenarios, albeit with a somewhat shallower  $[O/Fe]$  gradient than the default model of Pipino *et al.* (2006).<sup>5</sup>

Over the range  $1\lesssim R/R_{eff}\lesssim 5$ , the abundance (and abundance ratio) gradients in the hot corona of our simulated elliptical are  $d\langle[Fe/H]_X\rangle/d(\log r)\approx-0.6$  (a factor of two steeper than the iron gradient in the stellar component at  $R/R_{eff}\lesssim 1$ ) and  $d\langle[O/Fe]_X\rangle/d(\log r)\approx+0.1$  (which matches that of the stellar component at  $R/R_{eff}\lesssim 1$ , albeit, obviously offset by a factor of five in magnitude - see above), respectively. This abundance ratio is consistent with a scenario whereby  $\sim 70\%$  of the iron associated with the hot corona originated from Type Ia supernovae (Gibson *et al.* 1997).

<sup>4</sup>Also, for the first time, measured at  $R/R_{eff}\gtrsim 1$ .

<sup>5</sup>Which has a steeper gradient:  $d\langle[O/Fe]\rangle/d(\log r)\approx+0.3$ .

### 2.3 Metallicity Distribution Functions & Abundance Gradients

Using spatially-resolved metallicity distribution functions (MDFs) from HST, Harris & Harris (2002) infer a metallicity gradient for the stellar population of NGC 5128 of  $d(\langle [m/H] \rangle) / d(\log r_e) \approx -0.5 \text{ dex} / \log r$  (for  $1.4 \lesssim r_e \lesssim 4$ ); the FWHM dispersion of these empirical MDFs is  $\sim 1$  dex (see Fig 3). At the same effective radius, our simulated elliptical possesses a flat gradient in  $[m/H]$  (again, see Fig 3), matching such an inferred steep empirical slope only in the inner region of the galaxy (over the range  $0.2 \gtrsim r_e \gtrsim 0.5$  - recall Fig 2). This should not be surprising given that the simulation in question possesses gradients more broadly consistent with NGC 3379 (§ 2.2) than NGC 5128, but for illustrative purposes here the comparison remains of interest. Of perhaps more immediate interest though is the fact that the dispersion in the simulated MDFs is  $\sim 1.5$  dex (FWHM), a factor of 2-3 broader than the empirical MDFs. Whether this apparent discrepancy is a manifestation of a "G-dwarf" problem, contamination of the inner field MDF by a secondary bulge component, or partially driven by observational selection effects, remains unclear; what cannot be disputed though is the potential for future MDF observations to constrain elliptical galaxy formation scenario (Pipino *et al.* 2006).

## 3 Future Directions

While our past and ongoing work has proven successful across a range of testables, it is perhaps more interesting to emphasise here several of the unsolved problems, challenges, and potential pitfalls, remaining. For example, the observed abundances in the hot coronal gas of ellipticals are (roughly speaking) solar (for Fe, Mg, Si, S, and Ar), half-solar (O and Ne), and three times solar (Ni), while in the hot intracluster medium of galaxy clusters it is  $0.3 \times$  solar for Fe, twice solar for Si, half-solar for S, solar for Ni, and  $< 0.1 \times$  solar for Ar and Ca (with significant cluster-to-cluster variations). No combination of Type Ia and Type II supernovae can be made consistent with these data, implying the need for some additional metal source(s). That said, one remains constrained by empirical supernova rates now derived out to  $z \approx 1$ , while Pop III stars and hypernovae do not appear to be a panacea in this regard. Is the fact that our simulated MDF is  $\sim 0.5$  dex broader than the empirical MDF derived from NGC 5128 of concern? Is there a serious G-dwarf problem? How robust are our X-ray luminosity-weighted abundance and abundance ratio gradients at  $\sim 3 R_{eff}$ ? Is the line-of-sight velocity dispersion skewness  $h_3$  correlated with the sense of direction of the rotation velocity (Meza *et al.* 2003)? Are the optical and X-ray isophotes correlated in position angle and/or ellipticity? What impact might mass-dependent star formation and AGN feedback efficiencies play? Single simulations, such as that described here or in Meza *et al.* (2003), have proven enticing, but what is now needed is a significant statistical sample of cosmological elliptical galaxy simulations before we can properly address the nature of these empirical trends.

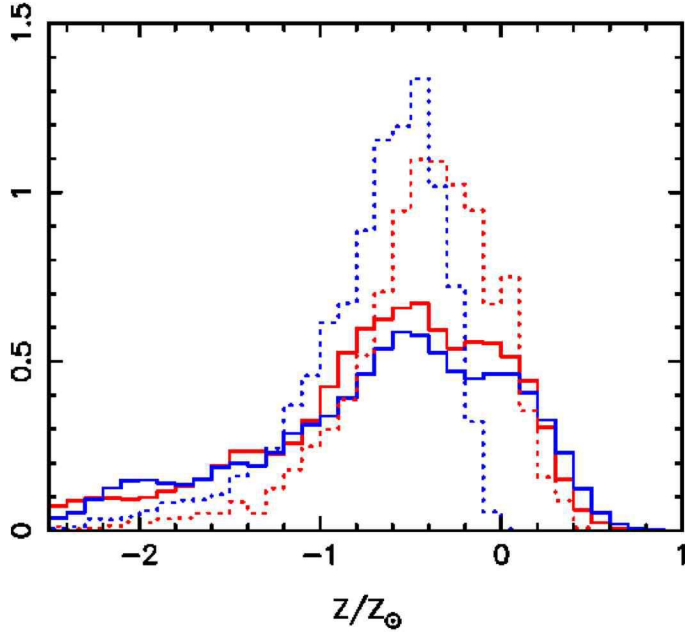


**Fig. 3.** Simulated (solid: Model 2 - Kawata & Gibson 2005) and empirical (dotted: NGC 5128 - Harris & Harris 2002) MDFs for the inner (red) and outer (blue) fields described in § 2.2.

## References

- Domínguez-Tenreiro, R., Onorbe, J., Sáiz, A., Artal, H. & Serna, A. 2006, *ApJ*, 636, L77  
 Gottlöber, S., Yepes, G., Khalatyan, A., *et al.* 2006, *astro-ph/0610622*  
 Gibson, B.K. 1997, *MNRAS*, 290, 471  
 Gibson, B.K., Loewenstein, M. & Mushotzky, R.F. 1997, *MNRAS*, 290, 623  
 Harris, W.E. & Harris, G.L.H. 2002, *AJ*, 123, 3108  
 Kawata, D. & Gibson, B.K. 2005, *MNRAS*, 358, L16  
 Kobayashi, C. 2004, *MNRAS*, 347, 740  
 Meza, A., Navarro, J., Steinmetz, M. & Eke, V. 2003, *ApJ*, 590, 619  
 Naab, T., Johansson, P.H., Ostriker, J.P. & Efstathiou, G. 2006, *astro-ph/0512235*  
 Pipino, A., Matteucci, F. & Chiappini, C. 2006, *ApJ*, 638, 739  
 Sánchez-Blázquez, P., *et al.* 2006, *MNRAS*, submitted  
 Sommer-Larsen, J., Götz, M. & Portinari, L. 2003, *ApJ*, 596, 47